4.6 Measured Dynamic Ranges

In both Techniques 1 and 2, the circuits are excited with two sinusoids at frequencies $f_1 = f_0 - 7.5$ kHz = 10.6925 MHz, and $f_2 = f_0 + 7.5$ kHz = 10.7075 MHz. The 3rd-order intermodulation (IM_3) products $|2f_1-f_2|$ and $|2f_2-f_1|$ are 10.6775 and 10.7225 MHz, respectively.

4.6.1 Measured Dynamic Ranges of Technique 1

Figure 4.11 shows the measured output spectrums of Technique 1 shown in Figure 3.2 at $Q_{HQ1} = 121$ using the two-frequency excitation of -20 dBm at f_1 and f_2. It can be seen that the IM_3 products are approximately 40 dB down from the fundamentals and correspond to 1% (or 1% IM_3).

Through a 50-Ω load of the spectrum analyzer without the output buffer, for Technique 1 shown in Figure 3.2, Figure 4.12 depicts the measured output levels (dBm) of the fundamental at f_1 and the IM_3 at $|2f_1-f_2|$ versus the input levels (dBm). The corresponding linear output levels are also included. It can be seen from Figure 4.12 that the noise power P_{N3} = –92.45 dBm and the third-order intermodulation intercept point IIP_3= 10 dBm. At the input level of –35 dBm, the output level of f_1 is –18 dBm whilst the output level of the IM_3 is adjacent to P_{N3} (or intermodulation free). Therefore the 3rd-order intermodulation-free dynamic range ($IMFDR_3$) = (–18 dBm) – (–92.45 dBm) = 74.45 dB. In addition, at the input level of –20 dBm, the output level of f_1 is –5 dBm, whilst the output level of the IM_3 is 40 dB down from f_1 (or 1% IM_3). Therefore, the wide dynamic range DR_1 (at 1% IM_3) = (–5 dBm) – (–92.45 dBm) = 87.45 dB which is relatively consistent with the expected value DR_1 = 88.28 dB predicted in Section 3.6 .

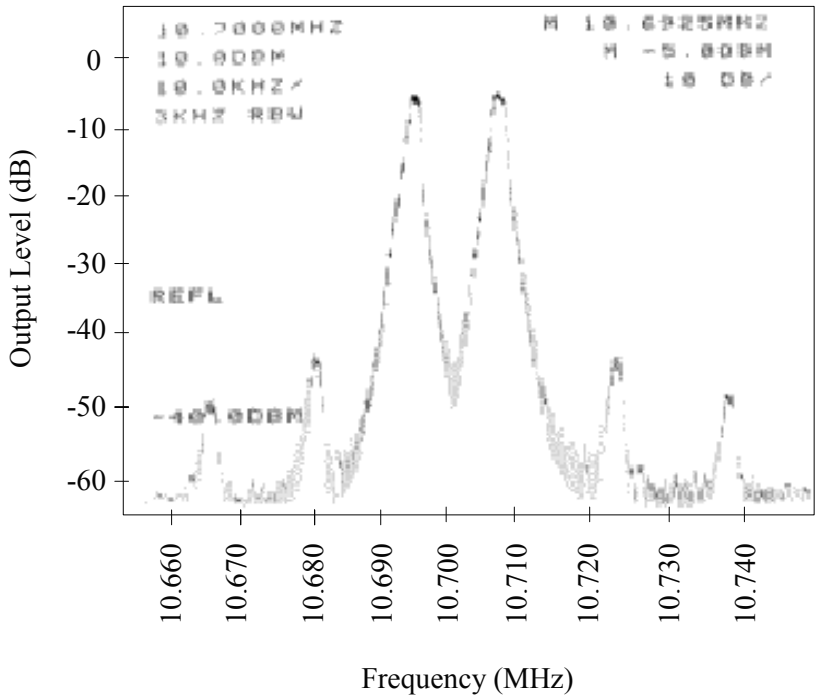

Figure 4.11 Measured output spectrums at the two-frequency excitation of –20 dBm of Technique 1 shown in Figure. 3.2.

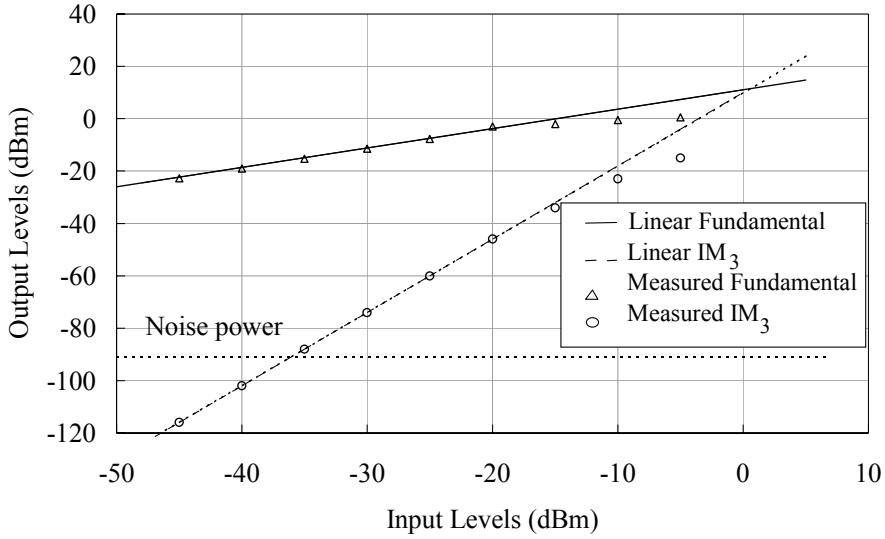

Figure 4.12 Measured output levels of the fundamental at f_1 and the IM_3 at $|2f_1-f_2|$ versus input levels of Technique 1 shown in Figure 3.2.

4.6.2 Measured Dynamic Ranges of Technique 2

Figure 4.13 shows the measured output spectrums of Technique 2 shown in Figure 3.3 at Q_{HQ2} = 223 using the two-frequency excitation of –20 dBm. It can be seen that the IM_3 products are also approximately 40 dB down from the fundamentals and therefore the IM_3 products are approximately 1% (or 1% IM_3).

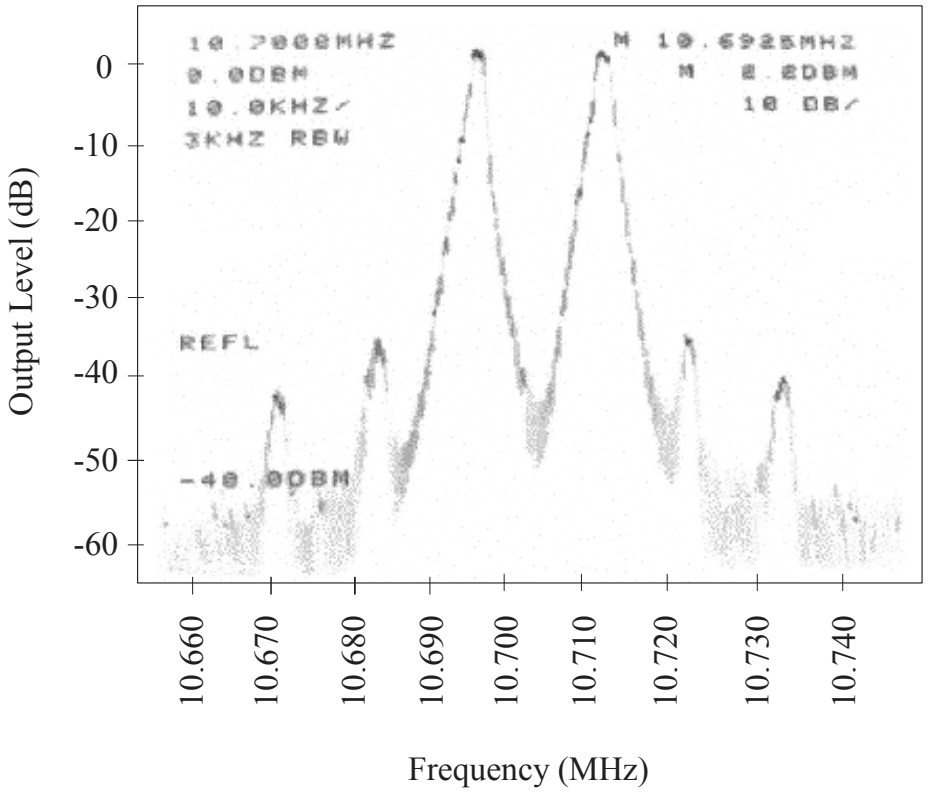

Figure 4.13 Measured output spectrums at the two-frequency excitation of –20 dBm of Technique 2 shown in Figure 3.3.

For Technique 2 shown in Figure 3.3, Figure 4.14, depicts the measured output levels (dBm) of the fundamental at f_1 and the IM_3 at $|2f_1-f_2|$ versus the input levels (dBm). The corresponding linear output levels are also included. It can be seen from Figure 4.14 that the noise power P_{N3} = –98.82 dBm and the third-order intermodulation intercept point IIP_3= -2

dBm. At the input level of –42 dBm, the output level of f_1 is –16 dBm whilst the output level of the IM_3 is adjacent to P_{N3} (or intermodulation free). Therefore the 3rd-order intermodulation-free dynamic range ($IMFDR_3$) = (–16 dBm) – (–98.82 dBm) = 82.82 dB. In addition, at the input level of –20 dBm, the output level of f_1 is 2.2 dBm, whilst the output level of the IM_3 is 40 dB down from f_1 (or 1% IM_3). Therefore, the wide dynamic range DR2 (at 1% IM_3) = (2.2 dBm) – (–98.82 dBm) = 101.02 dB.

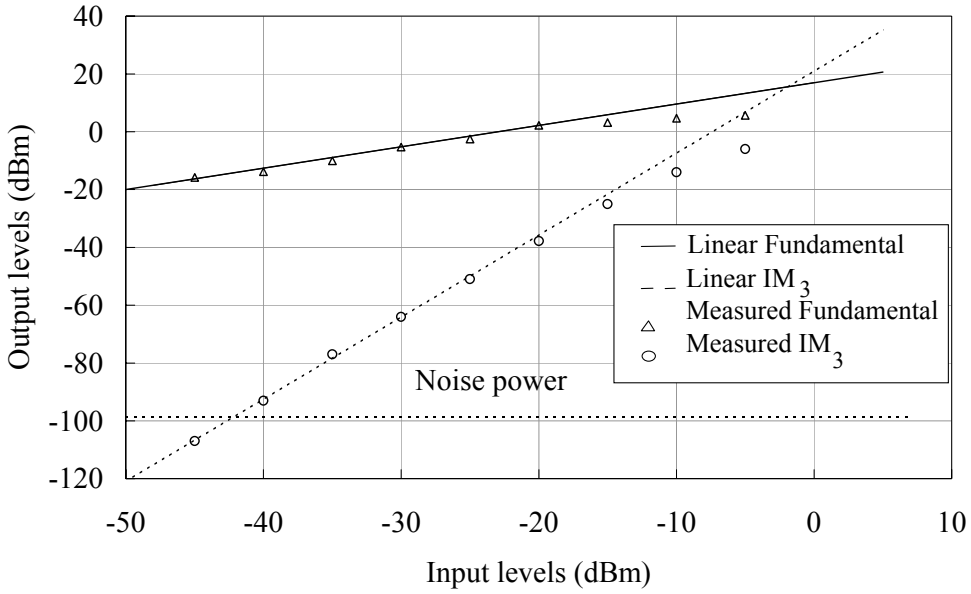

Figure 4.14 Measured output levels of the fundamental at f_1 and the IM_3 at $|2f_1-f_2|$ versus input levels of Technique 2 shown in Figure 3.3.

4.7 Temperature Compensation

4.7.1 Temperature Compensation for the Center Frequencies in Techniques 1 and 2

Figure 4.15 shows two cases of the measured variations of the normalized center frequency f_0 / (10.7 MHz) versus the ambient temperature (Celsius). The first case is an "uncompensated" case where the effects of temperature on the center frequency f_0 have not

been compensated. The second case is a "compensated" case where the effects of temperature on f_0 have been compensated.

The uncompensated case can be demonstrated by taking Figure 3.2 and 3.3 into an oven except that the connected two current sinks I_2 are located outside the oven (i.e. the two current sinks I_2 will be independent of the ambient temperature in the oven). It can be seen from Figure 4.15 that the normalized frequency of the "uncompensated" case decreases inversely with the ambient temperature (in the oven) as can be expected from (3.9) where effects of temperature caused by the thermal dependent voltage V_T is in the denominator of (3.9).

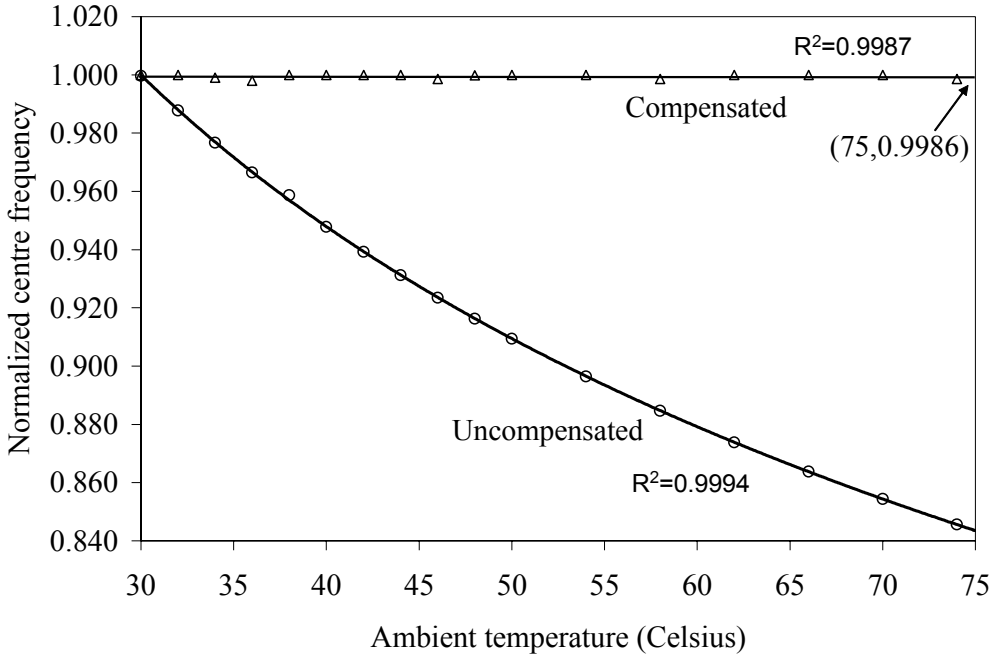

Figure 4.15 Normalized center frequencies versus ambient temperature for the uncompensated and compensated cases of Techniques 1and 2.

The compensated case can be demonstrated by taking Figure 3.2 and 3.3 into an oven including the connected two current sinks I_2 (i.e. the two current sinks I_2 will also be affected by the ambient temperature in the oven). It can be seen from Fig. 8 that the normalized frequency of the "compensated" case remains relatively constant, as can be expected from (3.9) where effects of temperature caused by V_T in the denominator of (3.9) can be compensated by the relatively similar effects caused by V_T of I_2 in the numerator of (3.9), i.e. $I_2 \propto v_{BE}$ where $v_{BE} = V_T \ln (I_c/I_s)$, I_c and I_s are the collector and saturation currents of a BJT in LM334.

In the compensated case, the temperature coefficients of the normalized center frequencies decrease drastically. The measured temperature coefficients for ambient temperature ranging from T_1 = 30 °C to T_2 = 75 °C are approximately –30 ppm/°C, i.e. $\cong [f(T_2) - f(T_1)] \times 10^6 / [f(T_1) \times (T_2 - T_1)] = (0.9986 - 1) \times 10^6 / [(1)(75 - 30)]$. The measurements have been obtained by putting the two frequency-determining capacitors outside the oven, and the measured temperature coefficients are therefore due to the intrinsic circuit parameters only.

4.7.2 Temperature Compensation for the Quality Factor Q_{HQ1} of Technique 1

Effects of temperature on the quality factor have never clearly been reported. In a similar manner to Section 4.7.1, Figure 4.16 shows two cases of the measured variations of the quality factor Q_{HQ1} versus the ambient temperature (Celsius), i.e. the uncompensated and the compensated cases. It can be seen from Figure 4.16 that Q_{HQ1} in the "uncompensated" case increases versus the ambient temperature as can be expected from (3.10) where β is proportional to temperature (Small-Signal Transistor Data, Philips Inc., 2001; Geiger and et

al., 1990). In addition, the variation of Q_{HQ} in the "compensated" case is reduced. Such variations of Q_{HQ} are not only gradually but also relatively much smaller and slower than the variations of most reported Q factors which have generally been a function of variables such as a center frequency or have particularly been inversely proportional to the center frequency (Bashar et al., 1996 and Ho-Kwang et al., 1996).

The measured temperature coefficients, ranging from T_1 = 30 °C to T_2 = 75 °C, are reduced approximately from 1,010 ppm/°C in the "uncompensated" case to 367 ppm/°C in the "compensated" case. As mentioned earlier, alternative solutions for good stability of the quality factor Q_{HQ} with temperature should be suggested through the use of special HBTs where good stability of β with temperature has been reported (Bashar et al., 1996 and Ho-Kwang et al., 1996).

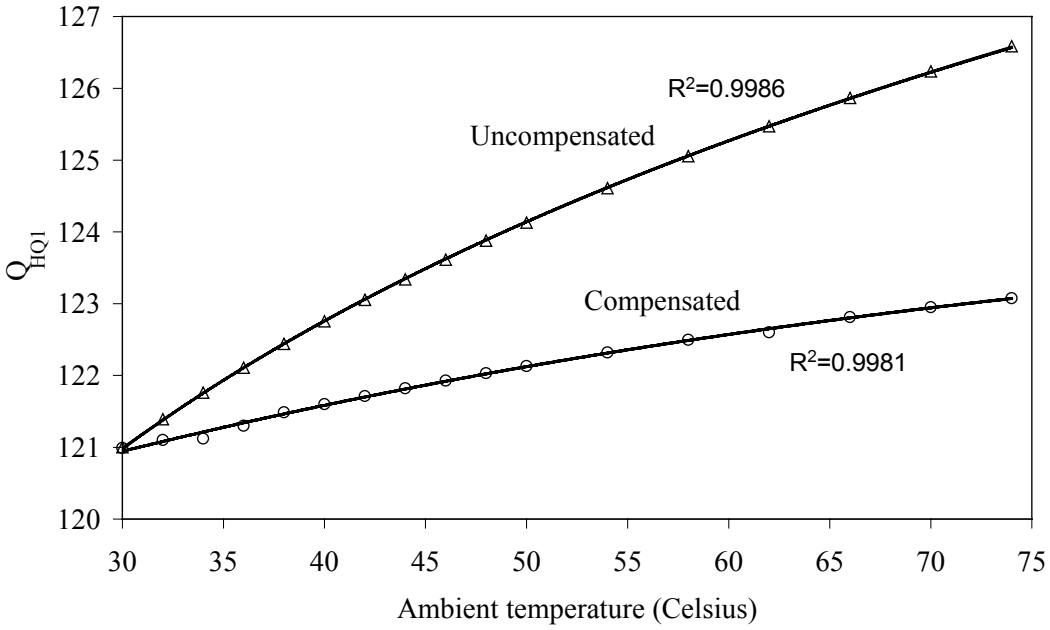

Figure 4.16 Variations of the quality factor Q_{HQ1} of Technique 1 shown in Figure 3.2 versus ambient temperature for the uncompensated and compensated cases.

4.7.3 Temperature Compensation for the Quality Factor Q_{HQ2} of Technique 2

As the ratio of I_3/V_T in (3.13) is in a similar manner to the ratio of I_2/V_T in (3.9), a similar temperature compensation can be expected for the quality factor Q_{HQ2} of Technique 2 described in (3.13). Figure 4.17 shows the measured variations of the quality factor Q_{HQ2} of Technique 2 shown in Figure 3.3 versus the ambient temperature (Celsius). In the uncompensated case shown in Figure 4.17, the current sink $2I_3$ is located outside the oven (i.e. temperature independent) and therefore Q_{HQ2} decreases inversely with the ambient temperature as can be expected from (3.13) where V_T is the thermal dependent in the denominator of the ratio I_3/V_T in (3.13). In the compensated case shown in Figure 4.17, the current sink $2I_3$ is included inside the oven (i.e. temperature dependent) and therefore the effects of the ambient temperature caused by V_T in the denominator are reduced or compensated by those caused by I_3 in the numerator of the ratio I_3/V_T in (3.13).

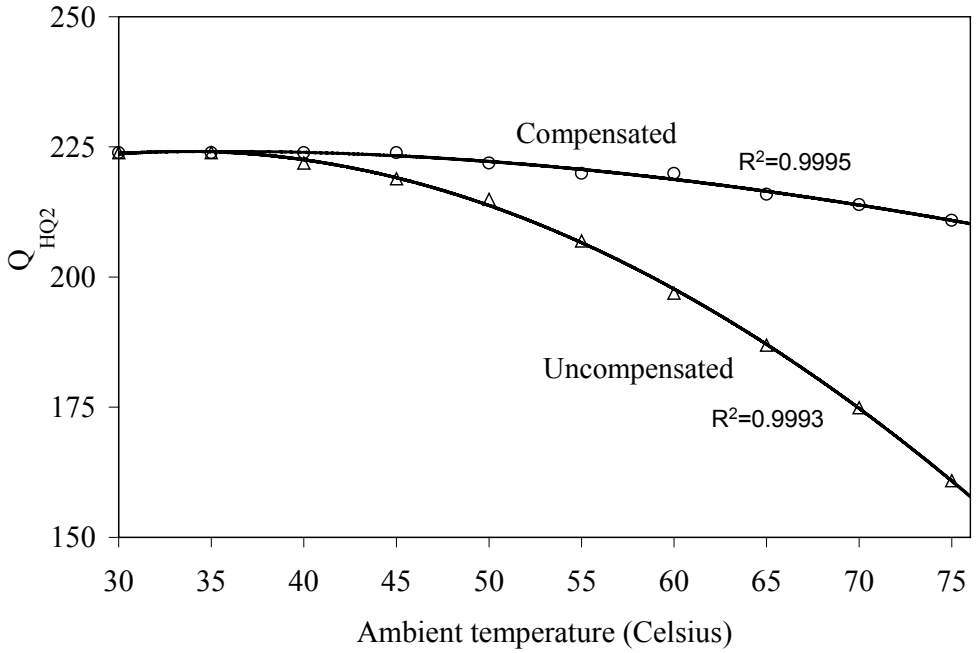

Figure 4.17 Variations of the quality factor Q_{HQ2} of Technique 2 shown in Figure 3.3 versus ambient temperature for the uncompensated and compensated cases.

Unlike the two cases in Figure 4.15 where the temperature dependent capacitors are located outside the oven, both cases in Figure 4.17 have been obtained by including the temperature dependent resistors $2R_c$ inside the oven. It may be observed from both cases in Figure 4.17 that the uncompensated effects of the ambient temperature due to the resistor R_c in the numerator of the ratio R_cI_3/V_T in (3.13) remain evident. The measured temperature coefficients, ranging from T_1 = 30 °C to T_2 = 75 °C, are reduced approximately from -3.33×10^5 ppm/°C to -1.4×10^6 ppm/°C.

4.8 Power Consumption Versus Dynamic Ranges

4.8.1 Preliminary Interpolation in Technique 1

Preferable requirements for an on-chip integrated bandpass filter include low power consumption, low silicon areas of capacitors, high dynamic ranges and high center frequencies whilst maintaining high quality factors. On the one hand, equation (3.9) suggests that not only the power consumption (P_{C1}) due to I_2 but also the silicon areas due to C_1, can be simultaneously reduced for the same ratio of (3.9). On the other hand, equation (3.14) suggests that the smaller the values of the capacitance in the circuit, the smaller the value of the dynamic range (DR1). As a result, higher dynamic ranges on chip require higher power consumptions and more silicon areas of capacitors.

As an example at the center frequency f_{01} = 10.7 MHz whilst maintaining the high quality factor Q_{HQ1} = 121, Figure 4.18 predicts preliminary interpolation of a power consumption P_{C1} and a corresponding dynamic range (DR1 at 1% IM_3) versus the capacitance C_1. It can be seen from Fig. 10 that a higher dynamic range DR1 = 87.45 dB requires a higher power consumption P_{C1} = 60 mW at C_1 = 150 pF, whilst a lower DR1 = 65.7 dB requires a lower P_{C1} = 0.4 mW at C_1 = 1 pF.

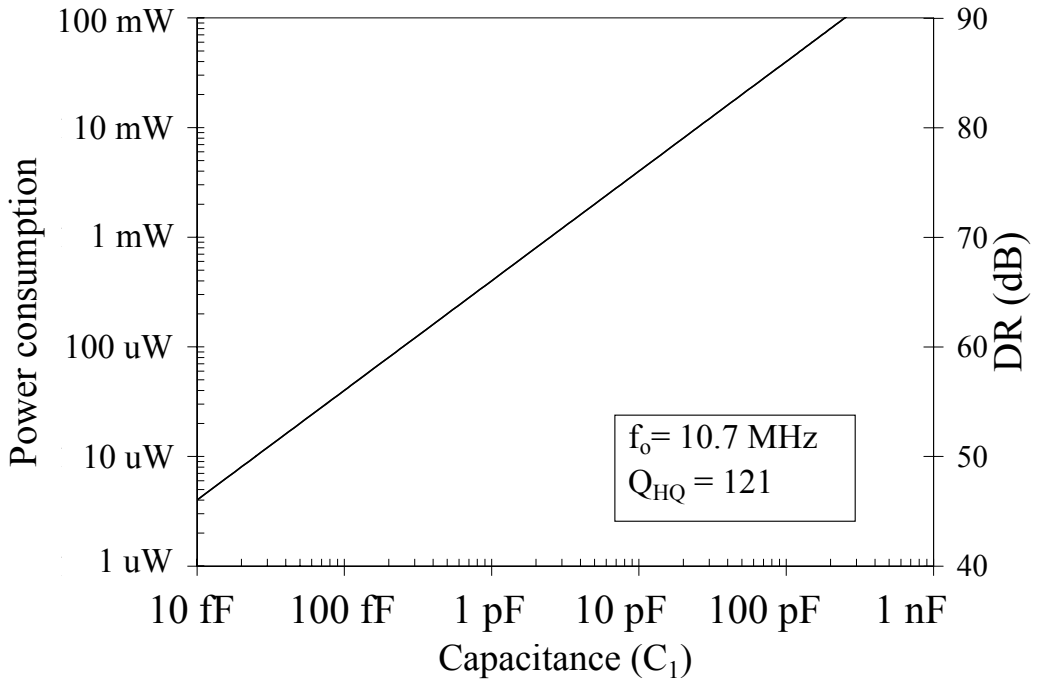

Figure 4.18 Preliminary interpolation of the power consumption (P_{C1}) and the dynamic range (DR1) of Technique 1 at 1% IM_3 versus C_1 at f_0 =10.7 MHz and Q_{HQ1} = 121.

4.8.2 Preliminary Interpolation in Technique 2

For Technique 2 shown in Figure 3.3, Figure 4.19 predicts preliminary interpolation of the power consumption P_{C2} and the dynamic range (DR2) at 1% IM_3 versus the capacitance C_1 at the center frequency f_0 = 10.7 MHz whilst maintaining the high quality factor Q_{HQ2} = 223. Figure 4.19 also suggests that the higher dynamic range (DR2) of 101.02 dB at C_1 = 150 pF and P_{C2} = 70 mW may be reduced to the lower dynamic range (DR2) of 80 dB at C_1= 1 pF and P_{C2} = 0.47 mW.